3-sphere fibrations: a tool for analyzing twisted materials in condensed matter

2009 J. Phys. A: Math. Theor. 42 465209

(http://iopscience.iop.org/1751-8121/42/46/465209)

IOP PUBLISHING JOURNAL OF PHYSICS A: MATHEMATICAL AND THEORETICAL

J. Phys. A: Math. Theor. **42** (2009) 465209 (17pp) doi:10.1088/1751-8113/42/46/465209

3-sphere fibrations: a tool for analyzing twisted materials in condensed matter

J F Sadoc and J Charvolin

Laboratoire de Physique des Solides, Université Paris-Sud, CNRS UMR 8502, F-91405 Orsay, cedex, France

E-mail: sadoc@lps.u-psud.fr

Received 29 May 2009, in final form 10 September 2009
Published 26 October 2009
Online at stacks.iop.org/JPhysA/42/465209

Abstract

Chiral molecules, when densely packed in soft condensed matter or biological materials, build organizations which are most often spontaneously twisted. The crystals of 'blue' phases formed by small mesogenic molecules demonstrate the structural importance of such a twist or torsion, and its presence was also recently observed in finite toroidal aggregates formed by long DNA molecules. The formation of these organizations is driven by the fact that compactness, which tends to align the molecules, enters into conflict with torsion, which tends to disrupt this alignment. This conflict of topological nature, or frustration, arises because of the flatness of the Euclidean space, but does not exist in the curved space of the 3-sphere where particular lines, its fibres, can be drawn which are parallel and nevertheless twisted. As these fibrations conciliate compactness and torsion, they can be used as geometrical templates for the analysis of organizations in the Euclidean space. We describe these fibrations, with a particular emphasis on their torsion.

PACS numbers: 61.30.Cz, 87.15.A, 02.40.k

1. Introduction

1.1. Torsion in dense media of chiral molecules

Typical manifestations of molecular chirality at the structural level are found in cholesteric and 'blue' liquid crystalline phases. These structures are built not only by small mesogenic molecules [1–3] but also by long biological macromolecules such as collagen fibrils [4, 5] and DNA [6, 7]. The field of molecular orientations in cholesteric phases can be described by a twist along successive parallel planes, the actual molecular locations being at random. In these phases, the twist is propagated along one direction only, that of the normal to the planes. In the 'blue' phases, the twist shows a tendency to be propagated uniformly around each

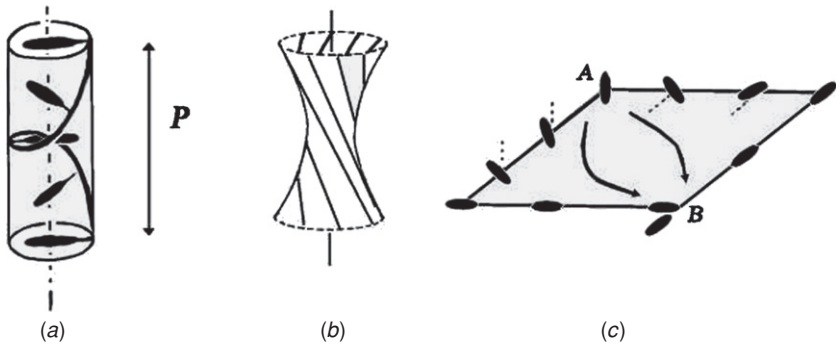

Figure 1. (*a*) Propagation of a twist along one direction only with pitch *P*. (*b*) A local view of the double twist situation. (*c*) The associated frustration on long distance; displacements obeying the double twist constraint along the two paths *AB* give incompatible molecular orientations in *B*.

molecule, or isotropically in the plane normal to the molecule, but this propagation cannot proceed as simply as in the cholesteric case, as shown in figure 1. If the molecules can arrange themselves with a uniform twist in the immediate vicinity of the molecule in A, molecules in B must have different orientations according to the path followed from A to B. The twist angle is not defined in B and the density of the medium is strongly perturbed in the vicinity of this point. The forces ensuring torsion and compactness are therefore in conflict, the system is said to be in a frustrated state. The structures of the 'blue' phases are those which conciliate these two terms in the best manner possible.

Whereas cholesteric and 'blue' phases are infinite structures, collagen [8] and DNA [9] are also able to build dense finite aggregates with a remarkable toroidal morphology under particular condensation conditions. We are currently examining if this toroidal morphology might also be considered as a solution optimizing a similar conflict between torsion and compactness. This analysis of 'blue' phase structures and toroidal aggregates (see part 6 for more details and references) relies on the so-called 'curved space approach' developed for describing frustrated systems [10], which proceeds in the following way. First, non-frustrated geometrical templates are built in non-Euclidean spaces which are chosen so that the two terms of the frustration are not in conflict. Then, the templates are mapped onto the Euclidean space by appropriate geometrical transformations. This approach provides a clear description of the distortions needed to optimize the frustration in real space. In the case of twisted materials considered here, the templates are built with fibrations of the curved space of the 3-sphere, the general mathematical framework of which is presented here.

1.2. The curved space approach

The frustration, which arises when the molecular orientation is transported along the two AB paths of figure 1, is imposed by the very topological nature of the Euclidean space R^3. It would not occur if the molecules were embedded in the non-Euclidean space of the 3-sphere S^3, or hypersphere. This space with a homogeneous positive curvature can indeed be described by equidistant and uniformly twisted fibres, along which the molecules can be aligned without any conflict between compactness and torsion. The stereographic projection in R^3 of the Hopf fibration in S^3 is represented in figure 2. The fibres of this fibration are great circles of S^3, the whole family of which is also called the Clifford parallels. Two of these fibres are C_∞ symmetry axes for the whole fibration; each fibre makes one turn around each axis and regularly rotates when moving from one axis to the other. These fibres build a double twist

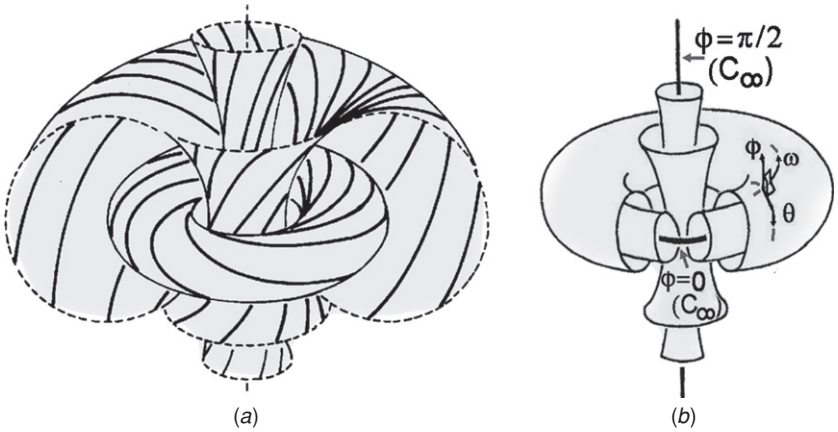

Figure 2. (*a*) Stereographic projection onto R^3 of some of the great circles of S^3. These circles are member of a family of the so called Clifford parallels which is also a Hopf fibration of S^3. (*b*) These fibres are supported by tori belonging to a S^3 torus 'foliation'. The two symmetry axes C_∞ are, before projection, two interlaced great circles of S^3.

configuration while staying parallel, i.e. without any frustration, in the whole volume of S^3 [11]. They can therefore be used as models to study the condensation of long molecules in the presence of a double twist constraint.

Of course these models embedded in S^3 have to be mapped onto R^3, an operation which cannot be made without distortion, whatever the method followed, as the first space is curved while the second is not. In the case of infinite structures, such as 'blue' phases, this is obtained by introducing lines of topological defects, disinclinations which balance, in R^3, the positive curvature of S^3. In the case of finite objects, such as toroidal aggregates, this is obtained using the stereographic projection. This transformation preserves topology, circles and angles so that the toroidal morphology and the rotation angle from one fibre to the other are not affected, but it introduces metric distortions so that the distance between molecules and the characteristic dimensions of the templates are modified by the projection. However these distortions remain weak, if not negligible, for the neighborhood of the $\phi = 0$ axis when projected from a pole on the $\phi = \pi/2$ axis.

Such an approach is justified by the fact that the energy of the configuration in the virtual space is minimal with regard to the double twist and compactness constraints, and that its mapping onto the real space introduces only the necessary distortions for the configuration to exist in this space. These distortions are localized along the disinclination lines of infinite structures or close to the surface of finite aggregates.

The Hopf fibration is only one among many in S^3; others making various numbers of turns around the axes have been proposed, known as Seifert fibrations, which can also be used to search for solutions to the conflict between compactness and torsion, at least in part of the S^3 volume. We examine here the properties of all these fibrations in view of such a use, with a particular emphasis on their torsion which appears to be an important factor in the organization of dense materials of chiral molecules.

2. The curved space of the 3-sphere

The 3-sphere is a curved 3-dimensional space described in 4-dimensional Euclidean space by the simple equation $x_1^2 + x_2^2 + x_3^2 + x_4^2 = R^2$. Two systems of coordinates, toroidal and

spherical, associated to its symmetries are currently used and, eventually, its representation by quaternions.

2.1. Toroidal coordinates

This system of coordinates is defined by:

$$\begin{aligned} x_1 &= R\cos\theta\sin\phi & x_2 &= R\sin\theta\sin\phi \\ x_3 &= R\cos\omega\cos\phi & x_4 &= R\sin\omega\cos\phi. \end{aligned} \tag{1}$$

with the angular parameters $\theta \in [0, 2\pi[$, $\phi \in [0, \pi/2]$ and $\omega \in [0, 2\pi[$.

Surfaces at constant ϕ are tori of the figure 2(*b*) organised around the two interlaced circles $x_1^2 + x_2^2 = R^2$ and $x_3^2 + x_4^2 = R^2$ corresponding to $\phi = \pi/2$ and $\phi = 0$ which are symmetry axes of S^3. The torus corresponding to $\phi = \pi/4$, the spherical or Clifford torus, is halfway between these two circles and divides S^3 in two congruent sub-spaces. The distance between two tori corresponding to ϕ and $\phi + d\phi$ is $R\,d\phi$ for all points of a torus so that the tori can be seen as equidistant 'parallel' layers in S^3 [12]. The element of area on torus ϕ is $ds = R^2\sin\phi\cos\phi\,d\theta\,d\omega$ so that the area of the torus is $4\pi^2R^2\sin\phi\cos\phi$, i.e. $2\pi^2R^2$ for the spherical torus. The fibres of S^3 are drawn on this family of tori defined by the angles ϕ.

2.2. Spherical coordinates

This system of coordinates is defined by:

$$\begin{aligned} x_1 &= R\cos\varpi & x_2 &= R\sin\vartheta\cos\varphi\sin\varpi \\ x_3 &= R\sin\vartheta\sin\varphi\sin\varpi & x_4 &= R\cos\vartheta\sin\varpi \end{aligned} \tag{2}$$

with the angular parameters $\vartheta \in [0, \pi[$, $\varphi \in [0, 2\pi[$ and $\varpi \in [0, \pi[$. Surfaces at constant ϖ are S^2 spheres of radius $R\sin\varpi$ centered on the points corresponding to $\varpi = 0$ and $\varpi = \pi$. The sphere corresponding to $\varpi = \pi/2$ with radius R, the great sphere, is at equal distance from these two points and divides S^3 in two congruent sub-spaces. The distance between two spheres defined by ϖ and $\varpi + d\varpi$ is $R\,d\varpi$ for all points of a sphere. The element of area on the sphere ϖ is $ds = R^2\sin\vartheta\sin^2\varpi\,d\vartheta\,d\varphi$ so that the area of the sphere is $4\pi R^2\sin^2\varpi$, i.e. $4\pi R^2$ for the great sphere. Although this system of coordinates does not correspond to the symmetry of the problem under study, it will prove to be useful when describing the torsion of the fibres.

2.3. Representation by quaternions

A circle, a 1-sphere, $x_1^2 + x_2^2 = r^2$, and the rotations on this circle are represented in a simple manner by a complex number $x_1 + \mathbf{i}x_2$ or $r\,e^{\mathbf{i}\theta}$ in the complex plane and the tangent vector to the circle is easily deduced as the product of this number with the pure imaginary number $\mathbf{i}$. The quaternions play the same role in the 3-sphere and are useful tools to express rotations in this space [13]. Quaternions are usually written with three imaginary unit numbers $\mathbf{i}, \mathbf{j}, \mathbf{k}$ in the form: $q = x_1 + x_2\mathbf{i} + x_3\mathbf{j} + x_4\mathbf{k}$, x_i being the coordinates of a point of the 3-sphere, the multiplication rules are defined by the Hamilton relations $\mathbf{i}^2 = \mathbf{j}^2 = \mathbf{k}^2 = \mathbf{ijk} = -1$ so that quaternions form a field $\mathbb{H}$ whose multiplication is not commutative. They can also be viewed as ordered pairs of complex numbers (s, t) and (u, v), where $s = x_1 + \mathbf{i}x_2$ and $t = x_3 + \mathbf{i}x_4$, with the following rules for addition and multiplication: $(s, t) + (u, v) = (s + u, t + v)$ and $(s, t)(u, v) = (su - t\bar{v}, sv + t\bar{u})$ where $\bar{u}$ is the complex conjugate of u. For instance, a torus ϕ in section 2.1. is described by the quaternion $(e^{\mathbf{i}\theta}\sin\phi, e^{\mathbf{i}\omega}\cos\phi)$.

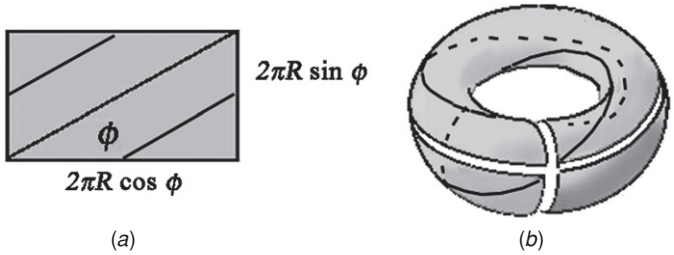

Figure 3. A rectangle (*a*) with edges of length of $2\pi R\cos\phi$ and $2\pi R\sin\phi$ is folded into a torus (*b*), by identification of its edges two by two, its diagonal, or any parallel line, becomes a great circle of S^3. Two such intertwined lines are shown in (*b*).

2.4. Tori and Clifford parallel lines

A torus ϕ is a surface without Gaussian curvature and with an Euclidean metric $dl^2 = \sum_{i=1}^{4} dx_i^2 = \frac{R^2}{2}(d\theta^2 + d\omega^2)$, it can therefore be considered as being built by identifications two by two of the sides of a rectangle with length $2\pi R\cos\phi$ and width $2\pi R\sin\phi$, or of a square in the case of the spherical torus, as shown in figure 3. These rectangles have a vanishing area for $\phi = 0, \pi/2$ and merge into the two great circles which are symmetry axes for the family of tori.

The diagonals of these rectangles, and their parallel lines, all have the same length $2\pi R$ and turn by an angle $d\phi$ when moving from torus ϕ to torus $\phi + d\phi$. They become great circles of S^3 after identifications of the sides of the rectangles. These great circles have no intersection, keep constant distances between them, and are interlaced, each one making one turn around the other and rotating by the angle $d\phi$ when moving from ϕ to $\phi + d\phi$. They are called Clifford parallels and we show below that they are also fibres of the Hopf fibration represented on figure 2. This simple representation of a torus as a rectangle with the fibres as the diagonals of this rectangle conveys two important points. First, in the system of toroidal coordinates with angular parameters θ, ω and ϕ, a great circle on torus ϕ is parameterized by one variable ω only, owing to the linear relationship $\theta = \omega + \omega_0$ existing between θ and ω along the diagonals. Second, as shown on figure 4, the great circles present a torsion angle $d\phi$ when their distance from the symmetry axis $\phi = 0$ increases by $R\,d\phi$.

However, in this representation related to the local frame (ϕ, θ, ω), this twist appears to be a simple one only, of the cholesteric type as shown in figure 4 although, intuitively, the transformation of the rectangle into a torus will contribute to the appearance of the double twist as suggested by the figure 3. We show latter that the choice of an adapted local frame demonstrates the existence of a double twist and makes its evaluation possible.

3. Fibrations of the 3-sphere

3.1. Definition of a fibration

A space can be considered as a fibre bundle if it contains a set of sub-spaces, the identical fibres, such that any point of the space is on only one fibre. A fibred space E is then defined by a mapping p from E onto a base B such that any point of a given fibre is represented by only one point on this base, i.e. a fibre is the full pre-image of one point of the base under p. In a 3-dimensional fibred space, the fibres are 1-dimensional spaces, lines, and the base is a 2-dimensional space, a surface. For example, the Euclidean space R^3 can be considered as a

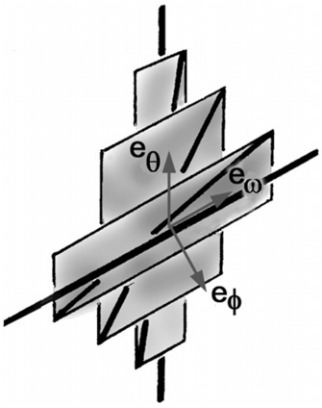

Figure 4. Representation of a family of tori by parallel rectangles whose diagonals will become Clifford parallel, or Hopf fibres, after identifications two by two of the sides of the rectangles. In the local frame (e_θ and e_ω parallel to the sides of the rectangles, e_ϕ normal to them) associated with variations of toroidal coordinates, only a simple twist of the cholesteric type is apparent.

fibre bundle of parallel straight lines R^1 all perpendicular to the same plane R^2; the base is then a sub-space of the fibred space and the fibration is said to be trivial. This is not always the case, particularly with the fibrations of S^3.

3.2. Hopf fibration

The family of Clifford parallels described just above fulfils the requirements of the preceding definition. This is the Hopf fibration such that S^3 can be seen as a bundle of parallel great circles S^1 represented on a spherical base S^2 built in R^3, a non-trivial fibration. A great circle of the 3-sphere S^3 with radius R can be seen as the orbit of the isometry $q \longrightarrow e^{i\alpha}q$ with $\alpha \in [0, 2\pi[$ and where q is the quaternion of a point in S^3 which can be written as a pair of complex numbers (u, v) such that $u\bar{u} + v\bar{v} = R^2$. The base of the fibration with great circles, the Hopf fibration, is then be built resulting from the composition of the map h_1 from S^3 onto the complex plane R^2 (with ∞ included) with the inverse stereographic projection h_2 from R^2 onto S^2:

$$\begin{aligned} &h_1 : S^3 \longrightarrow R^2 \\ &(u, v) \longrightarrow Q = uv^{-1} \qquad \text{with} \quad u, v \in \mathbb{C} \\ &h_2 : R^2 \longrightarrow S^2 \\ &Q \longrightarrow M = (y_1, y_2, y_3) \qquad \text{with coordinate} \quad y_i \in \mathbb{R}. \end{aligned} \tag{3}$$

As a great circle is the orbit of the isometry $(u, v) \longrightarrow (e^{i\alpha}u, e^{i\alpha}v)$, applying h_1 to any point of it results in a complex number $Q = u/v$ which has always the same value whatever α and therefore is characteristic of the whole circle. Moreover, the base thus obtained is a 2-sphere embedded in R^3 but not in S^3, if it was, it would be intersected by a fibre in two points, as a circle always cuts a sphere in two points, and this would go against the definition which requires that a fibre is represented by one point of the base only. The coordinates and properties of the spherical base are deduced in the following way.

The angles ϕ, θ, ω of the toroidal coordinates defining a point (u, v) of a fibre with $u = R\,e^{i\theta}\sin\phi$ and $v = R\,e^{i\omega}\cos\phi$, the point Q obtained in the complex plane by the map

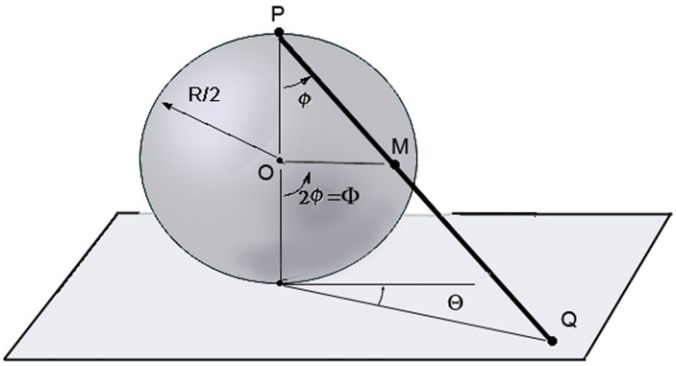

Figure 5. Inverse stereographic projection h_2 from the complex plane onto the spherical base S^2. The radius $R/2$ has been choose so that the distances on the base are equal to the distances between corresponding fibres.

h_1, is defined by the complex number $Q = e^{\mathbf{i}(\theta-\omega)} \tan\phi$ with modulus $\rho = \tan\phi$ and phase $\Theta = (\theta - \omega)$, then the point M obtained on a sphere with radius 1/2 by the map h_2 has the following coordinates:

$$y_1 = \tfrac{1}{2}\cos(2\phi) \qquad y_2 = \tfrac{1}{2}\sin(2\phi)\sin\Theta \qquad y_3 = \tfrac{1}{2}\sin(2\phi)\cos\Theta \qquad (4)$$

as shown in figure 5.

Thus, the point M defined by the spherical coordinates Θ and $\Phi = 2\phi$ is representative of a great circle parameterized by $\theta = \omega + \Theta$ and $\phi = \Phi/2$ and the Clifford parallels are the fibres of the Hopf fibration admitting the sphere as a base. The correspondence between the coordinates of the fibres in S^3 and these of their representative points on the S^2 base can be summarized as:

$$(\theta, \phi, \omega) \longrightarrow (\Phi, \Theta)$$

with $\Phi = 2\phi$, $\Theta = \theta - \omega \in \lfloor 2\pi \rfloor$, $\Phi \in [0, \pi[$, $\Theta \in [0, 2\pi[$. A torus of the family of nested tori supporting the Clifford parallel or fibres being defined by a constant angle ϕ, the two poles $\Phi = 0$ and π of this sphere are representative of the symmetry axes $\phi = 0$ and $\pi/2$ of the family, its equator $\Phi = \pi/2$ corresponds to the spherical torus $\phi = \pi/4$ and all other tori are represented by parallels.

The radius R of the 3-sphere, defining length scale, does not appear in the coordinates of the base, the representative 2-space for fibres, so its realization can be done with a 2-sphere of any radius. Nevertheless, there is an interesting choice adding a factor R in the (y_1, y_2, y_3) coordinates of the base which then becomes a 2-sphere of radius $R/2$. Doing so, the distance $R\,\mathrm{d}\phi$ between two tori in S^3 is that of their two representative parallels $R/2\,\mathrm{d}\Phi$ measured along a great circle of the base. This can be generalized for the distance between two fibres in S^3 which is exactly that between two points on the base.

3.3. Seifert fibrations

Fibres of the Hopf fibration are characterized by the fact that they make one turn around each of the axes of the family of their supporting tori, but the very nature of the system under study may require fibrations with different numbers of turns. For instance, our analysis of toroidal aggregates of DNA [14] was developed with fibres making one turn around one axis but up to six turns around the other. For this use we were therefore led to consider the whole set of

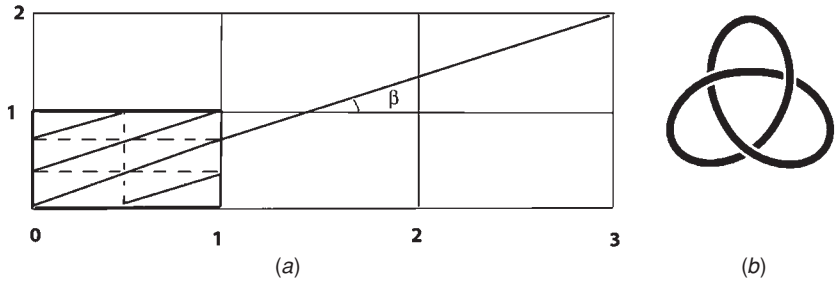

Figure 6. (*a*) Drawing of a {3, 2} fibre on the rectangle representative of a torus of constant ϕ in S^3. The fibre is first drawn as the diagonal of a large rectangle of coordinates (3, 2), then the segments of the fibre appearing in the small rectangles are transfered within the rectangle of coordinates (1, 1) chosen to represent the torus. (*b*) This fibre has the topology of the trefoil knot.

other fibrations of S^3 in a topological sense, known as Seifert fibrations, which includes the Hopf fibration. Publications on Seifert fibrations mainly focus on topological questions and are not directly applicable to condensed matter structures, some interesting information were found in [15–18]. We introduce these fibrations following the line of the development used above for the Hopf fibration. We define a topological fibration as a mapping on a base of topologically equivalent fibres with, in the present case, two singular fibres defined by $\phi = 0$ and $\pi/2$.

Seifert fibres are such that they make k turns around the axis $\phi = \pi/2$ and l turns around the axis $\phi = 0$, a configuration henceforth noted $\{k, l\}$. The trajectory of a $\{3, 2\}$ fibre on its supporting torus unfolded as a rectangle, and the way it is obtained, is shown in figure 6. This is an helix drawn on a torus. If the construction of figure 6 is used to draw a $\{3, 3\}$ fibre, it appears that all the replicas of the segments of the diagonal of the (3, 3) rectangle are superimposed as three $\{1, 1\}$ fibres in the (1, 1) rectangle representative of the torus. Similarly, a $\{6, 4\}$ fibre appears as two $\{3, 2\}$ fibres. A unique fibre is obtained only when k and l have no common divider except 1, i.e. are coprime numbers.

Fibres are defined as the orbit of an isometry applied to a point of the 3-sphere, written here as a quaternion q

$$q \longrightarrow e^{i(\frac{k+l}{2})\alpha} \cdot q \cdot e^{i(\frac{l-k}{2})\alpha} \tag{5}$$

with $\alpha \in [0, 2\pi]$. This isometry is, with the quaternion q given as a pair of complex numbers, $(u, v) \longrightarrow (e^{il\alpha}u, e^{ik\alpha}v)$.

Consider a fibre $\{k, l\}$ drawn on a torus making k turns around its axis defined by $\phi = \pi/2$, and l turns around the other axis defined by $\phi = 0$. On the torus unfolded into a rectangle, it appears as line segments which are parallel to the diagonal of a large rectangle with side length k and l time those of the rectangle representing the torus, as shown on figure 6. On this torus, the equation of a line characterized by ω_0 is $\theta = l\omega/k + \omega_0$ and its β angle with a rectangle edge is given by $k \tan\beta = l \tan\phi$ as $\tan\phi$ is the ratio of rectangle edge lengths. A point on a 2-surface can represent it because this line is defined by two parameters ϕ and ω_0 as in the Hopf fibration case.

3.3.1. Base of the Seifert fibration. In the case of the Hopf fibration, we have emphasized the fact that the distance between two fibres is also the distance between the two representative points on the base (with radius $R/2$). Using the classical definition of a geodesic distance between two curves in the 3-sphere, we hope to have the same property for the Seifert base.

We define the following application of a point $q = (u, v)$ of a fibre on the complex plane:

$$(u, v) \longrightarrow Q = \frac{u^k}{v^l} \qquad \text{with} \quad u, v \in \mathbb{C}. \tag{6}$$

Clearly with this choice, all points of the same fibre give the same point in the complex plane.

On the torus characterized by the angular parameter ϕ, there is a fibre through the point with angular coordinates (ϕ, θ, ω), represented by the quaternion $(u, v) = (e^{il\alpha} e^{i\theta} \sin\phi, e^{ik\alpha} e^{i\omega} \cos\phi)$. The path along this fibre is covered when α varies from 0 to 2π. The complex number $Q = e^{i(k\theta - l\omega)} \frac{(\sin\phi)^k}{(\cos\phi)^l}$, has the same modulus $\rho = \frac{(\sin\phi)^k}{(\cos\phi)^l}$ for all fibres of the torus, not depending from θ and ω which characterize the position of fibres on the torus. Then in the complex plane fibres are given by Q with modulus ρ and phase $\Theta = k\theta - l\omega$.

Distances in the complex plane are defined by length element δl with a metric $\delta l^2 = d\rho^2 + \rho^2 d\Theta$. But this metric is not such that the distance between two points equals the distance between the two corresponding fibres. It has to be changed in order to obtain this property. The new metric induces the shape of the base.

3.3.2. Metric of the Seifert base. The distance between two fibres on two different tori contains two terms:

- the distance $R\, d\phi$ between the two tori,
- the distance between two fibres on the same torus.

In the complex plane these two terms correspond to variations of the modulus ρ for the first one, and of the Θ phase for the second.

The first step to evaluate the distance between two fibres of the same torus consists in determining the distance between two spires of the same fibre. This distance, $L(\phi)$, is such that, from figure 6, the area of the torus $4\pi^2 R^2 \sin\phi\cos\phi = L(\phi)\lambda_f$ where the length of the fibre is $\lambda_f = 2\pi R\sqrt{k^2\cos^2\phi + l^2\sin^2\phi}$. Thus

$$L(\phi) = 2\pi R \frac{\sin\phi\cos\phi}{\sqrt{k^2\cos^2\phi + l^2\sin^2\phi}}. \tag{7}$$

This distance is measured on the surface of the torus along its geodesics. But a geodesic of the torus is not a geodesic of the 3-sphere because on a torus unfolded into a rectangle, the straight line along which the distance is measured does not fold into a great circle. Nevertheless, the aim is not to get the distance between two spires of the same fibre, but the infinitesimal distance between two close fibres defined on the torus by Θ and $\Theta + d\Theta$. This distance is proportional to $L(\phi)$. Using the fact that the fibre defined by Θ is also defined by $\Theta + 2\pi$, we get the infinitesimal distance between two close fibres: $(L(\phi)/2\pi)\, d\Theta$. In other words, integrating this from 0 to 2π at constant ϕ gives the length of the circle with radius ρ, but the true distance between two spires of the same fibre will need to have a variable ϕ in order to follow a geodesic line.

The wanted metric is then:

$$\begin{aligned} \delta l^2 &= R^2 \left(d\phi^2 + \left(\frac{L(\phi)}{2\pi} \right)^2 d\Theta^2 \right) \\ \delta l^2 &= R^2 \left(d\phi^2 + \left(\frac{\sin\phi\cos\phi}{\sqrt{k^2\cos^2\phi + l^2\sin^2\phi}} \right)^2 d\Theta^2 \right). \end{aligned} \tag{8}$$

In the case, $\{k, l\} = \{1, 1\}$ corresponding to the Hopf fibration, this metric takes the form $\delta l^2 = d\phi^2 + (\sin\phi\cos\phi)^2 d\Theta^2$ or $\delta l^2 = \frac{1}{4}[d(2\phi)^2 + \sin^2(2\phi)\, d\Theta^2]$, with $R = 1$ for simplicity,

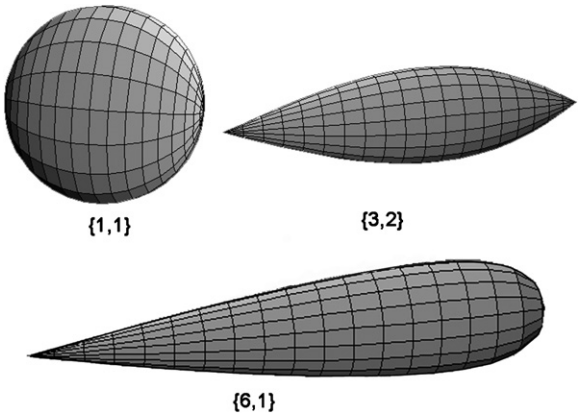

Figure 7. Bases parameterised in ϕ, varying from 0 (left) to $\pi/2$ (right), for $\{1, 1\}$, $\{3, 2\}$ and $\{6, 1\}$ fibrations. These surfaces are determined by the position $R\phi$ of a point along a meridian and the radius $(R \sin\phi \cos\phi)/\sqrt{k^2 \cos^2\phi + l^2 \sin^2\phi}$ of the parallel going through that point.

which is the same as the metric for a 2-sphere with radius $1/2$ defined by angular parameters $\Phi = 2\phi$ and Θ. The modification of the complex plane metric thus induces the metric of the 2-sphere base. For the Seifert fibration, there are two singular fibres for $\phi = 0$ and $\phi = \pi/2$ which appear as singularities of the metric. The metric in the vicinity of $\phi = 0$, with $R = 1$, can be approximated by $\delta l^2 \approx \mathrm{d}\phi^2 + \frac{\phi^2}{k^2}\,\mathrm{d}\Theta^2$ which has a conical singularity at the origin if $k > 1$. This happens also for $\phi = \pi/2$ at the other pole of the base if $l > 1$.

So, in the example of Hopf fibration the metric imposed to the complex plane induces the metric of the spherical base, for Seifert fibration the imposed metric induced the metric of a surface of revolution shown on figure 7.

4. Tools used to study torsion in the 3-sphere

The torsion between two fibres of a bundle is characterized by the angle made by their tangent vectors at two points of the bundle which depends on the length and orientation of the vector joining these two points. In Euclidean space, a simple parallel transport of the local frame from one point, with its tangent vector, to the other point allows it to compare the orientation of the two tangent vectors within the same frame. The procedure in a curved space is similar but requires a more elaborated analysis as several rules of transport of local frames are possible according to the definition of connections in differential geometry [19].

4.1. Local frames in the 3-sphere

A vector and its representation by coordinates in a frame can be defined only in Euclidean space. In a curved space this is defined in a Euclidean space that best approximates the local space, i.e. the tangent space at the point where the vector is. This position in a 3-sphere is given by a quaternion $q = (x_1, x_2, x_3, x_4)$ whose four elements are written using toroidal or spherical coordinates. For simplicity the 3-sphere radius is taken to $R = 1$, so that quaternions are unit quaternions. The transport from point-to-point of a local frame can be related to the choice of the coordinate system or not. In the first case they are called natural frames. In the

following we use two local natural frames associated with toroidal and spherical coordinates of the 3-sphere. We also use a non-natural frame directly associated to quaternions.

4.1.1. Local frame associated to pure imaginary quaternions. It is well known that in the complex plane a circle with unit radius is characterized by the complex number $r\,e^{\mathbf{i}\theta}$ with $r = 1$, and a tangent vector to the circle is obtained by product with the pure imaginary number $\mathbf{i}$. In the space of quaternions, similar things occur. A 3-sphere with a unit radius is characterized with a unit quaternion q and the three numbers $e_i = \mathbf{i}\cdot q$, $e_j = \mathbf{j}\cdot q$ and $e_k = \mathbf{k}\cdot q$ obtained by products with the three pure imaginary numbers ($\mathbf{i}$, $\mathbf{j}$, $\mathbf{k}$) are characterizing vectors of the tangent space to the 3-sphere at point q. Nevertheless, it is important here to note that the product by pure imaginary numbers that are on the left as multiplication of quaternions is not commutative. The quaternions (e_i, e_j, e_k) characterize unit vectors. Using Hamilton rules for quaternion multiplication it appears that these three vectors are orthogonal, so they define an orthonormal basis for a local frame also called (e_i, e_j, e_k), as throughout this paper we use quaternions as points of the 3-sphere, but also as coordinates of vectors in the tangent space.

4.1.2. Frame associated to spherical coordinates. In the plane it is possible to define also the tangent vector to a unit radius circle by derivation of the polar coordinates relatively to the angular variable. Similarly, in R_4 vectors of the tangent space at points of a 3-sphere, can be obtained from spherical coordinates $(\vartheta, \varpi, \varphi)$ by angular derivatives. Spherical coordinates in R_4 are given in equation (2). If these four coordinates are gathered into a quaternion $q(\vartheta, \varpi, \varphi)$, three quaternions characteristic of vectors of the tangent space, are derivatives of q with respect to the spherical angular coordinates ϑ, ϖ and φ. After normalization these three quaternions are:

$$\begin{aligned} e_\vartheta &= \frac{1}{\sin\varpi}\partial_\vartheta q(\vartheta, \varpi, \varphi) \\ e_\varpi &= \partial_\varpi q(\vartheta, \varpi, \varphi) \\ e_\varphi &= \frac{1}{\sin\varpi\,\sin\vartheta}\partial_\varphi q(\vartheta, \varpi, \varphi). \end{aligned} \tag{9}$$

The three corresponding vectors also form an orthonormal basis for a local frame called $(e_\vartheta, e_\varpi, e_\varphi)$.

4.1.3. Frame associated to toroidal coordinates. Toroidal coordinates are given in equation (1). These coordinates, gathered into the quaternion $q(\theta, \omega, \phi)$ can be used to define in the 3-sphere tangent space, three vectors by derivation with respect to the angular quantities θ, ω and ϕ:

$$\begin{aligned} e_\theta &= \frac{1}{\sin\phi}\partial_\theta q(\theta, \omega, \phi) \\ e_\omega &= \frac{1}{\cos\phi}\partial_\omega q(\theta, \omega, \phi) \\ e_\phi &= \partial_\phi q(\theta, \omega, \phi). \end{aligned} \tag{10}$$

These vectors are normalized in order to defined an orthogonal basis of a new local frame $(e_\theta, e_\omega, e_\phi)$.

4.2. Vectors expression in local frames

As we describe the 3-sphere in four-dimensional space, it is convenient to write vectors of tangent space in four dimensions. This will complete the local frames of the tangent three-

dimensional space with another vector in an extra dimension orthogonal to it. This fourth basis vector e_r is the radial vector characteristic of the point position on the 3-sphere. Then a transformation matrix allows us to change coordinates of a vector $\vec{v} = (v_1, v_2, v_3, v_4)$, written in the Cartesian R_4 global frame into coordinates in the local frame. For practical reasons the four elements of quaternions are expressed using toroidal coordinates whatever the local frame is.

The new coordinates of the $\vec{v}$ vector expressed in the basis (e_r, e_i, e_j, e_k) associated to pure imaginary quaternions, are obtained from the Cartesian coordinates, written as a column matrix by $M_{\text{im}}.\vec{v}$, where the matrix M_{im} is:

$$\begin{pmatrix} \cos\theta\sin\phi & \sin\theta\sin\phi & \cos\phi\cos\omega & \cos\phi\sin\omega \\ -\sin\theta\sin\phi & \cos\theta\sin\phi & -\cos\phi\sin\omega & \cos\phi\cos\omega \\ -\cos\phi\cos\omega & \cos\phi\sin\omega & \cos\theta\sin\phi & -\sin\theta\sin\phi \\ -\cos\phi\sin\omega & -\cos\phi\cos\omega & \sin\theta\sin\phi & \cos\theta\sin\phi \end{pmatrix}. \tag{11}$$

The new coordinates of the $\vec{v}$ vector expressed in the basis $(e_r, e_\theta, e_\omega, e_\phi)$ associated to toroidal coordinates, are $M_{\text{tor}} \cdot \vec{v}$, where the matrix M_{tor} is:

$$\begin{pmatrix} \cos\theta\sin\phi & \sin\theta\sin\phi & \cos\phi\cos\omega & \cos\phi\sin\omega \\ -\sin\theta & \cos\theta & 0 & 0 \\ 0 & 0 & -\sin\omega & \cos\omega \\ \cos\theta\cos\phi & \cos\phi\sin\theta & -\cos\omega\sin\phi & -\sin\phi\sin\omega \end{pmatrix}. \tag{12}$$

The new coordinates of the $\vec{v}$ vector expressed in the basis $(e_r, e_\vartheta, e_\varpi, e_\varphi)$ associated to spherical coordinates, are $M_{\text{sph}} \cdot \vec{v}$, where the matrix M_{sph} is:

$$\begin{pmatrix} \cos\theta\sin\phi & \sin\theta\sin\phi & \cos\phi\cos\omega & \cos\phi\sin\omega \\ -A & \frac{\cos\theta\sin\theta\sin^2\phi}{A} & \frac{\cos\theta\cos\omega\sin\phi\cos\phi}{A} & \frac{\cos\theta\sin\omega\sin\phi\cos\phi}{A} \\ 0 & -\frac{\cos\phi}{A} & \frac{\cos\omega\sin\theta\sin\phi}{A} & \frac{\sin\theta\sin\phi\sin\omega}{A} \\ 0 & 0 & -\sin\omega & \cos\omega \end{pmatrix}. \tag{13}$$

with $A = \sqrt{1 - \cos^2\theta\sin^2\phi}$. If we are interested with vectors that are tangent to fibres, so in the tangent space the first coordinate in local frames must be null as it corresponds to the dimension added orthogonally to the tangent space.

5. Torsion angle between fibres

The existence of a double twist in the fibre bundle of a fibration can be inferred from figure 2 in a rather simple way. The fibres drawn on a torus defined by an angle ϕ appear to be at an angle $\mathrm{d}\phi$ from those drawn on a parallel torus defined by $\phi + \mathrm{d}\phi$. This is also valid for two fibres drawn on this torus ϕ as, owing to the isometry of the fibres which have all the same environment, they can be considered similarly in another family of tori with different axes in the 3-sphere. Figure 2 thus suggest an isotropic torsion around each Hopf fibre whose angle increases with the distance between two fibres.

However, this is only a cursory approach to the description of the torsion as it does not make apparent the fact that the view one may have indeed depends on the choice of the transported local frames. This dependance must be examined, particularly because it cannot be avoided in the case of Seifert fibrations.

5.1. Torsion in hopf fibration

The Hopf fibrations can be defined using quaternions. A circular fibre is the trajectory of a q_0 point under the action of a quaternion $e^{\mathbf{i}\alpha}$, with α from 0 to 2π. Then a unitary vector tangent to the fibre at q_0 is characterized by the quaternion $\frac{\partial(e^{\mathbf{i}\alpha}q_0)}{\partial\alpha} = \mathbf{i}\cdot q_0$ with $\alpha = 0$. Element of this quaternion are components in R_4 of the tangent vector. We then express this vector in local frames to compare tangent vectors of different fibres.

5.1.1. Tangent vector in the frame associated with pure imaginary numbers. The (e_i, e_j, e_k) frame is given by $\mathbf{i}\cdot q_0, \mathbf{j}\cdot q_0$ and $\mathbf{k}\cdot q_0$ at q_0 point. So in this frame the tangent vector is simply $(1, 0, 0)$ for all points.

The conclusion comes directly: in this case there is no torsion, as in a parallel field of vectors. In fact this means that the frame is transported from point-to-point parallel to the fibration. This is the reason why Hopf fibres are sometime called 'Clifford parallels'. Notice here that the two vectors e_j and e_k are not tangent to the surface of the torus defined by ϕ. When the frame runs along a fibre these vectors always directed orthogonally to the fibre twist around it.

5.1.2. Tangent vector in the frame associated to toroidal coordinates. The tangent vector to a fibre through a point q_0 with toroidal coordinates θ_0, ω_0, ϕ is $t(q_0) = \mathbf{i}\cdot q_0$. This is the quaternion $\{-\sin\theta_0 \sin\phi, \cos\theta_0 \sin\phi, -\cos\phi \sin\omega_0, \cos\phi \cos\omega_0\}$, whose four elements form a column matrix $t(q_0)$ allowing us to get the tangent vector coordinates in the local frame by $M_{\text{tor}} \cdot t(q_0)$. This coordinates are $\{0, \sin\phi, \cos\phi, 0\}$; the first one is null as expected for a vector in the tangent space.

These coordinates do not depend on θ_0 and ω_0 angles which characterize the position of a point on a fibre lying on the torus defined by ϕ. So all tangent vectors to fibres on the same torus have the same coordinates. Using the local frame obtained from toroidal coordinates, fibres on a given torus are parallel lines. But two fibres on two different torus ϕ and $\phi + \mathrm{d}\phi$ have tangent vectors rotated by $\mathrm{d}\phi$. There is a torsion when ϕ change. In the 3-sphere, using toroidal coordinates to define a local frame, Hopf fibres behave like a cholesteric phase: the field of tangent vectors is parallel in layered tori and twist in the orthogonal direction to them.

5.1.3. Tangent vector in the frame associated to spherical coordinates. Consider two close fibres, which are at constant distance from each other, with a point q_0 on one fibre and a point q_1 on the other fibre, in such way that the distance between the two points is the distance between fibres; the torsion per unit length is defined by the angle between the two tangent vectors at these two points divided by their distance. We consider this distance as infinitesimal. Although the local frame is derived from spherical coordinates it is more convenient to characterize a fibre passing through a point $q_u = (\theta_u, \omega_u, \phi)$ with $(u = 0, 1)$ using the writing of toroidal coordinates. This is given by $\{\cos(\theta - \theta_u)\sin\phi, \sin(\theta - \theta_u)\sin\phi, \cos(\theta - \omega_u)\cos\phi, \sin(\theta - \omega_u)\cos\phi\}$, the θ angle being variable, the tangent vector at q_u is $\mathbf{i}\cdot q_u$. Without loss of generality, we set for q_0, $\theta_0 = 0$ and $\omega_0 = 0$. For the choice of q_1 there are two possibilities: q_1 on the same torus defined by ϕ than q_0, or on a parallel torus defined by $\phi + \mathrm{d}\phi$. In this second case, toroidal coordinates for q_1 are $\theta_1 = 0, \omega_1 = 0, \phi + \mathrm{d}\phi$ and the distances between the two points and between the two fibres are equal to $\mathrm{d}\phi$. In the first case, q_1 is chosen on the same torus as q_0 at an infinitesimal distance ϵ with q_1 toroidal coordinates $\theta_1 = -\epsilon\cot\phi, \omega_1 = \epsilon\tan\phi$ and ϕ. Applying the M_{sph} matrix to tangent vectors at these points give components of tangent vectors in the local frame related to spherical coordinates, $(e_r, e_\vartheta, e_\varpi, e_\varphi)$:

$\{0, 0, -\sin\phi, \cos\phi\}$ for the fibre through q_0 in the torus defined by ϕ;
$\{0, 0, -\sin(\phi + d\phi), \cos(\phi + d\phi)\}$ for the fibre on a close torus defined by $\phi + d\phi$;
$\{0, \frac{\sin\phi \sin(\epsilon \cot\phi)}{\sqrt{1-\cos^2(\epsilon \cot\phi)\sin^2\phi}}, -\frac{\sin\phi\cos\phi\cos(\epsilon\cot\phi)}{\sqrt{1-\cos^2(\epsilon\cot\phi)\sin^2\phi}}, \cos\phi\}$ for the fibre on the same torus than q_0.

The two first vectors coordinates show that they make a $d\phi$ angle. The cosine of the angle between the first vector and the last one is deduced from the scalar product of these vectors using the above coordinates. In the limit of an infinitesimal ϵ, this cosine is $1 - \frac{\epsilon^2}{2}$ related to an angle ϵ.

In the two cases we found that the torsion angle goes as the distance. This was the intuitive result given above, but to obtain this result we have to use a local frame whose transport rule is related to spherical coordinates. How do we explain this? The 3-sphere space is indeed isotropic with the same metric properties in all directions, nevertheless the choice of a local frame with a transport rule can break this isotropy. For instance the set of local frames associated to toroidal coordinates does not have the entire symmetry of the 3-sphere, but only a set of continuous rotation along the two great circles represented by the two opposite poles on the Hopf base ($\phi = 0, \phi = \pi/2$). In the case of local frame (e_i, e_j, e_k), the symmetry is a screw symmetry. It is only with the local frame $(e_\vartheta, e_\varpi, e_\varphi)$ associated with spherical coordinates that the transport rule retains the isotropic symmetry of the 3-sphere. It is only with this choice that it is possible to appreciate the real torsion.

5.2. Torsion in Seifert fibrations

Seifert fibres which are topologically equivalent but not isometric (they are identical on one torus but not from one torus to another) do not allow a simple cursory approach similar to that used in the case of Hopf fibres and we move directly to the description of the torsion by transport of the tangent vectors in the three local frames. As in the case of Hopf fibres, it appears that only the local frame associated to spherical coordinates provides a complete access to torsion angles.

The local frame associated to pure imaginary quaternions is strongly related to the Hopf fibration. When transporting this frame along a Hopf fibre the e_i vector remains tangent to the fibre, and orthogonal e_j and e_k vectors have a screw displacement. This frame is not very fruitful for Seifert fibrations.

In the local frame associated to toroidal coordinates it appears simply that fibres in the same torus are parallel lines. Fibres in different tori, like in the Hopf case appear as a cholesteric. But their direction are characterized by an angle β which depends on ϕ as $\tan\beta = (l/k)\tan\phi$ for a $\{k, l\}$ fibre. So the torsion angle is $\frac{l\,d\phi}{k}$ for two fibres at distance $d\phi$ on two different tori if ϕ remains small.

The torsion has to be evaluated in the local frame associated to spherical coordinates. The equation for a $\{k, l\}$ Seifert fibre defined on a torus by the angle ϕ in toroidal coordinates, through the point q_0 with $(\theta_0, \omega_0, \phi)$ coordinates is:

$$\{\cos(l\theta + \theta_0)\sin\phi, \sin(l\theta + \theta_0)\sin\phi, \cos(k\theta + \omega_0)\cos\phi, \cos\phi\sin(k\theta + \omega_0)\}.$$

The tangent vector to this fibre is obtained by derivation relatively to θ. Then it is expressed in the local frame $(e_r, e_\vartheta, e_\varpi, e_\varphi)$. Following this, three vectors are determined. The first one, as reference, passes through the point q_0 with $(\theta_0, \omega_0, \phi) = (0, 0, \phi)$ using toroidal coordinates. There is another one, on a close torus through the point $q_2 = (0, 0, \phi + d\phi)$ in order to have the torsion for a displacement normal to torus. The third one is in the same torus ϕ through the q_1 point at a ϵ infinitesimal distance from q_0. It appears that the variation of the torsion angle for fibres on the two tori ϕ and $\phi + d\phi$ is $\frac{kl\,d\phi}{k^2 sin^2\phi + l^2\cos^2\phi}$ which is for small ϕ: $\frac{l\,d\phi}{k}$, approximately

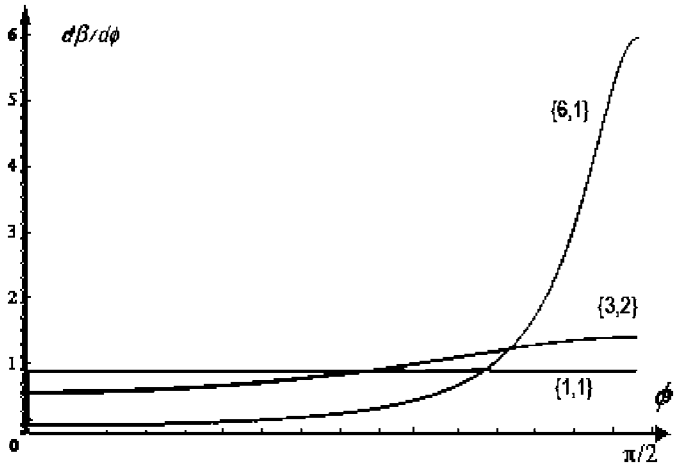

Figure 8. Torsion $\mathrm{d}\beta/\mathrm{d}\phi$ as a function of the position defined by ϕ, where $\mathrm{d}\beta$ is the angle between two close fibres (see figure 6) for {1, 1}, {3, 2} and {6, 1} fibrations. As the torsion is isotropic it is also $R\,\mathrm{d}\beta/\epsilon$ where ϵ is the infinitesimal distance between two fibre being ϵ. For the $\{k, l\} = \{6, 1\}$ case, the torsion is $l/k = 1/6$ in the limit of small ϕ and it is $k/l = 6$ in the limit of $\phi = \pi/2$.

independent of ϕ. For fibres in the same torus this angle is $\frac{\epsilon kl}{k^2 sin^2\phi + l^2\cos^2\phi}$, so the torsion is the same for displacement inside or orthogonal to tori. So for small ϕ, the torsion angle vary like l/k, but conversely to the Hopf fibration case, this is not true for large ϕ. Nevertheless, if the torsion changes with the ϕ position as shown in figure 8 it remains isotropic.

6. Physical examples

The double twist notion was introduced for the description of blue phases. These liquid crystals having cubic symmetries, with crystallographic groups $P4_232$ and $I4_132$ and large crystal cells of the order of 100 nm, are formed with small mesogenic molecules in a small region of the phase diagram between cholesteric phases and isotropic liquid [20]. Following this description, molecules build cylinders of double twist packed such that the cubic symmetries are respected and that director orientations are the same on the surface of cylinders at their points of contact. If the double twist condition is well respected in the cylinders and propagate from cylinder-to-cylinder through their contacts, strong discrepancies appear out of the cylinders where directors are organized around disclination lines. This model analyzes a blue phase as an entanglement of two cubic networks: one formed by cylinder axes, locally surrounded by double twist, and one formed by lines of defect relaxing the frustration of the twist locally. A presentation in terms of a director field with an uniform twist using parallel transport rules allows us to have a more continuous view of the structure in which the disclination lines allow the mapping in the Euclidean space of a {1, 1} Hopf fibration respecting the double twist condition perfectly in the 3-sphere [11]. All these works on blue phases are presented in [2, 3].

The {1, 1} Hopf fibration is also used in the analysis of the first step of the fibrils formation of collagen, the main constituent of conjunctive tissues [22]. Simple left polypeptide helices are gathered in a triple right helix to built collagen molecules then assembled into fibrils. The description of the core of the triple helix thus obtained is in good agreement with structural data demonstrating the importance of hydrophobic interaction in the stabilization of this helix.

Even if many works have been carried out in order to understand the fibril formation [5], it is not clearly possible to confirm the role of the double twist, but there are examples of simple twist with cholesteric phases [23]. To our knowledge the only indication of double twist can be deduced from the formation of fibrils, with toric organization, precipitated from collagen molecules [8]. With these observations, by Cooper, and the energetic argument he has developed, fibrils could be seen as stereographic projections of {1, 1} Hopf fibration in the 3-sphere. It was also shown that in particular physicochemical conditions, fibrils precipitate in micro-metric finite domains showing double twist very close to a stereographic projection of {1, 1} Hopf fibration [4].

Finally, DNA provides good examples of the use of Seifert fibrations. DNA can be wrapped, *in vitro* and *in vivo*, into dense toric aggregates whose size is about 10 nm [9]. This very particular form of compaction is considered by several authors as a fundamental morphology chosen by nature for preserving DNA before transcription. The thermodynamical stability of these aggregates has been studied in the frame of theoretical works on polyelectrolytes and liquid crystals, but starting *a priori* from the toric shape. Supposing that the DNA chirality impose a twist and using the {6, 1} Seifert fibration in a curved space approach we show that its shape must be toric and its size close to the observed size [14]. The need for this Seifert fibration, with a more complex topology than the Hopf fibration used for the above examples has been confirmed recently by a study of toric aggregates inside viral capsids partially filled by DNA [21].

7. Conclusion

We have examined the fibrations of the curved space of the 3-sphere to determine to which extent they can be used as geometrical templates with perfect long range order for analyzing infinite structures or finite aggregates of densely packed chiral molecules. The formation of these organizations in our Euclidean space is dominated by a conflict between alignment and torsion whose solutions implies the presence of structural defects or a limited growth. Perfectly ordered templates are starting points to appreciate how the introduction of defects or the control of the growth make these formations possible.

This examination has required a detailed analysis of parallel transport of local frames in the curved 3-sphere. Three different local frames are used, associated to quaternions, related to toroidal or spherical coordinates, each one emphasizing a particular property of a fibre bundle in such space: the parallelism of Hopf fibres with the first, the cholesteric state of Hopf and Seifert fibres on the tori foliation of the space with the second, and the existence of an isotropic double twist around each fibre with the third. However, all fibrations of the 3-sphere are not equivalent in the sense that, if the value of the double twist remains constant within the whole curved space in the case of the Hopf fibration, this is only in a limited part of it for all Seifert fibrations when their basis can be approximated by a cone.

These fibrations provide therefore a remarkable set of templates among which a choice can be made in order to obtain the closest adaptation to the requirements of the real systems as far as topology, intermolecular distance, torsion and characteristic dimensions are concerned.

Our presentation of fibrations calls upon mathematics relatively familiar to condensed matter physicists, except perhaps ‘quaternions’ which are nevertheless not too far from complex numbers. But other concepts developed to study the topology of manifold [24] could be used as well. The unit 3-sphere is a 3-dimensional manifold, having a group structure well represented by quaternions on which it is possible to draw vector fields without singularity. For this reason it is a Lie group and the vectorial algebra in tangent space is a Lie algebra. In this presentation we have often considered points in the 3-sphere and vectors in the tangent space as represented

by quaternions or described in well defined local frames. This is the benefit of the Lie algebra structure which allows us to represent objects as different as symmetry operations and vectors with a quaternion number continuously defined.

8. Acknowledgments

We thank Pierre Pansu (Département de mathématiques, Université de Paris-Sud, Orsay) for illuminating discussions about Seifert fibrations.

References

[1] de Gennes P G 1974 *The Physics of Liquid Crystals* (Oxford: Clarendon)
[2] Wright D C and Mermin N D 1989 *Rev. Mod. Phys.* **61** 385
[3] Pansu B and Dubois-Violette E 1990 *J. Phys. (Paris)* **51** C7–281
[4] Bouligand Y, Denefle J P, Lechaire J P and Maillard M 1985 *Biol. Cell* **54** 143
[5] Gaill F 1990 *J. Phys. (Paris)* **51** C7–169
[6] Leforestier A and Livolant F 1994 *Liquid Crystals* **17** 651
[7] Pelta J, Durand D, Doucet J and Livolant F 1996 *Biophys. J.* **71** 48
[8] Cooper A 1969 *Biochem. J.* **112** 515
[9] Hud N V and Downing K H 2001 *Proc. Natl Acad. Sci. USA* **98** 14925
[10] Sadoc J F and Mosseri R 1999 *Geometrical Frustration* (Cambridge: Cambridge University Press)
[11] Sethna J, Wright D C and Mermin N D 1983 *Phys. Rev. Lett.* **51** 467
[12] Coxeter H S M 1973 *Regular Complex Polytopes* (Cambridge: Cambridge University Press)
[13] du Val P 1964 *Homographies, Quaternions and Rotations* (Oxford: Clarendon)
[14] Charvolin J and Sadoc J-F 2008 *Eur. Phys. J.* E **25** 335
[15] Seifert H and Threlfall W 1934 Lehrbuch der Topologie Teubner, Leipzig, (Translated into English) 1980 *A Textbook of Topology and Seifert: Topology of 3-dimensional Fibered Spaces* (New York: Academic)
[16] Birman J S and Williams R F 1983 *Topology* **22** I-47
[17] Frank H and Lutz F H 2003 *ZIB-Report* **03-36**
[18] Pansu P Private communications
[19] Dandoloff R and Mosseri R 1987 *Europhys. Lett.* **3 11** 1193
[20] Meiboom S, Sammon M and Berreman D W 1983 *Phys. Rev.* A **28** 3553
[21] Leforestier A and Livolant F 2009 *Proc. Natl Acad. Sci. USA* **106** 9157
[22] Sadoc J-F and Rivier N 1999 *Eur. Phys. J.* B **12** 309
[23] Giraud-Guille M-M 1988 *Calcif. Tissue Int.* **42** 167
[24] Thurston W P 1980 *The Geometry and Topology of Three-Manifolds* (notes distributed by Princeton University) or Electronic version 1.1 (http://www.msri.org/publications/books/gt3m/)